Proceedings of the 6th Annual ISC Graduate Research Symposium
ISC-GRS 2012
April 13, 2012, Rolla, Missouri

COMPRESSIVE SENSING FOR WIDEBAND SAR IMAGING SYSTEMS

Hamed Kajbaf **Yahong Rosa Zheng**

Electrical and Computer Engineering Department
Missouri University of Science and Technology
Rolla, MO 65409
{hamed.kajbaf, zhengyr}@mst.edu

ABSTRACT

In this paper the adaptive basis selection (ABS) compressed sensing method is proposed. In contrast to conventional compressed sensing with fixed sparsifying basis, the proposed ABS method adapts the basis to the image as the image is evolved during the iterations of the algorithm. In this method the sparsifying basis is selected from a set of bases based on the information from incomplete measurements without any *a priori* knowledge of proper basis. The algorithm benefits from the ability to search through a diverse set of bases for unknown signals. A decision metric is introduced based on the sparsity of the image and the coherence between the measurement and sparsifying matrices. This decision metric makes the adapting process possible for practical applications. The results of our experiments show that the proposed algorithm is capable of recovering 2D synthetic aperture radar (SAR) images very well without compromising the complexity of the recovery process.

1. INTRODUCTION

Sparse representation and compressibility of signals have been studied very well under data coding in past years. Transform coding has shown very interesting results in sparsely representing signals and is widely used in data compression. Recently, compressed sensing theory has combined the approach of first sampling the signal and then compressing it by measuring the signal with the rate of sparsity [1]-[3]. In compressed sensing theory, sub-Nyquist sampling of a signal is achievable by utilizing sparse representation of the signal using an orthogonal basis.

Consider a signal $\mathbf{f} \in \mathrm{C}^N$ and its transform coding $\mathbf{c}$ with an orthonormal basis $\mathbf{\Psi} = \begin{bmatrix} \boldsymbol{\psi}_1 & \boldsymbol{\psi}_2 & \cdots & \boldsymbol{\psi}_N \end{bmatrix}$ such that $\mathbf{f} = \mathbf{\Psi c}$. If most of the information of the signal $\mathbf{f}$ is contained in only a few elements of the transformed signal $\mathbf{c}$, the signal $\mathbf{f}$ is called S *-sparse* in basis $\mathbf{\Psi}$ if only S of its coefficients are significant and the rest $N-S$ coefficients are zero. Therefore, a fixed signal support T of size $|T| = S$ can form an S *-sparse* signal. In other words,

$$S = \|\mathbf{c}\|_0 \tag{1}$$

where $\|\cdot\|_0$ is the ℓ_0 pseudo-norm operator and counts the nonzero elements of the coefficients $\mathbf{c}$.

In compressed sensing, the sparsity of the signal is used to sample the signal $\mathbf{f}$ more efficiently by measuring $M < N$ linear combinations of the signal. Let us define measurement matrix $\mathbf{\Phi}_\Omega \in \mathrm{R}^{M \times N}$ by selecting the rows of a measurement matrix $\mathbf{\Phi} \in \mathrm{R}^{N \times N}$ on a set $\Omega \subset \{1,2,\cdots,N\}$ with the size $|\Omega| = M$ where $\mathbf{\Phi}$ is modeling the linear measurement procedure. The linear measurement procedure can be modeled in matrix form as

$$\mathbf{y} = \mathbf{\Phi}_\Omega \mathbf{f} \tag{2}$$

where $\mathbf{y}$ is the measured signal. The inverse problem is to recover the original signal from linear measurements. In general, this inverse problem is underdetermined and there are infinite solutions which satisfy (2). In compressed sensing, the sparsity of the signal is used to find a unique sparse solution for this problem.

Compressed sensing is similar to decoding procedure in transform coding as both estimate the signal by applying the inverse of encoder orthonormal basis $\mathbf{\Psi}$ on the sparse coefficients $\mathbf{c}$ supported on set T. CS differs from transform coding as the location of support T and the value of the coefficients at these locations c_T is unknown. The only known variable is a sampled linear combination of the signal.

The same as in data compression, proper sparse representation in CS is very essential for accurate recovery of the signal. Conventionally, a fixed basis is use in CS to recover the data from incomplete measurement. In this scenario, it is assumed that we know the proper basis in advance. This assumption is not very accurate for many practical applications especially when we have an incomplete set of data available.

Dictionary learning and best basis selection compressed sensing are proposed in the literature to address this issue by evolving the best basis during the recovery procedure [4]-[9]. These methods systematically develop a dictionary without any assumption of a global sparse representation. In this way the dictionary adapts itself to the signal as the signal is recovered using CS. The systematic approach for learning a dictionary or

selecting bases is usually used to decrease the complexity of basis searching algorithms. However, the algorithm loses diversity of search and requires some assumption on sparse representation of the signal.

In this paper a new adaptive basis selection (ABS) algorithm is proposed to address the issue of selecting a proper basis without compromising the complexity of the recovery process. In this approach, the proper basis is selected from a set of bases according to its sparsifying capability and its incoherence with measurement domain. As the signal is recovered iteratively and a more accurate estimation of the signal is available, the algorithm selects the proper basis more accurately. The proposed method can benefit from a divers set of bases. In other words, for an unknown signal, a divers set of bases can be used for better sparse representation and consequently increasing the chance of recovery.

1.1. Application

For a perfect recovery of an unknown signal, we need to know the sparsifying basis from only incomplete measurements. For the applications where the desired signal is not changing sparsity characteristics for different experiments, a proper basis can be determined in advance. This can be done by calibrating the recovering process using a given test signal for one experiment in different basis and comparing the recovered signals. For other experiments, we use a fixed basis as determined in the calibration procedure, assuming that the sparsity characteristics are not changed. This assumption is not always accurate and the adaptive basis selection compressed sensing is proposed in this paper to address this issue. In this paper, the application of the proposed method is presented for synthetic aperture radar (SAR) imaging for nondestructive testing of materials and the performance and results are discussed.

Microwave SAR imaging is a high resolution technique which can be exploited to detect discontinuities in critical structures by raster scanning a specimen under test (SUT) using a single antenna probe (e.g. an open-ended waveguide). The scanning procedure is very time consuming and for a relatively large SUT might be hours of data acquisition. It is shown that random spatial measurements can be used to significantly reduce the acquisition time. The signal is then recovered using ℓ_1 norm minimization with different orthogonal bases [10], [11]. The drawback is that the proper sparsifying basis is determined by trying different basis and choosing the one with best SAR image quality. This approach is not desired in practice as the proper basis could be different for different SUTs. In contrast, adaptive basis selection approach chooses the proper basis iteratively as the signal is evolved using ℓ_1 norm minimization. This application is discussed in details in Section 4.

2. FIXED BASIS AND BEST BASIS CS FOR IMAGE PROCESSING

2.1. Fixed Basis

The sparsity of the signal helps solving the system of equations (2) by searching for the sparsest coefficients $\mathbf{c}$ which matches the incomplete measurement signal $\mathbf{y}$. By defining $\mathbf{A} = \mathbf{\Phi\Psi}$ and $\mathbf{A}_\Omega = \mathbf{\Phi}_\Omega\mathbf{\Psi}$, this can be formulated as

$$\min_{\mathbf{c}\in C^N} \|\mathbf{c}\|_1 \quad \text{s.t.} \quad \mathbf{y} = \mathbf{A}_\Omega\mathbf{c}. \tag{3}$$

Convex optimization (3) is guaranteed to recover $\mathbf{f}$ with high probability from linear measurements if some conditions are satisfied [12]. The minimum number of linear measurements guaranteeing perfect recovery is related to the sparsity of the signal and the coherence between the measurement and sparsifying bases. The coherence $\mu(\mathbf{\Phi},\mathbf{\Psi})$ between the measurement matrix $\mathbf{\Phi}$ and transform matrix $\mathbf{\Psi}$ is defined as

$$\mu(\mathbf{\Phi},\mathbf{\Psi}) = \sqrt{N}\max_{1\le u,v\le N} \left|\langle \boldsymbol{\varphi}_u, \boldsymbol{\psi}_v \rangle\right| \tag{4}$$

which is an indication of how correlated the measurement and the sparsifying bases are.

For a 2D signal if variation of the signal are very sharp with small variation in the background, finite differences is usually used as a sparsifying transform. The objective function in (3) is then replaced by total variation (TV). The TV penalized objective function can be combined with other sparsifying bases and can be interpreted as requiring the image to be sparse by both the specific basis and finite differences at the same time. In this case (3) can be written as [13]

$$\min_{\mathbf{c}\in C^N} \lambda_\ell \|\mathbf{c}\|_1 + \lambda_t \mathrm{TV}(\mathbf{\Psi c}) + \|\mathbf{y} - \mathbf{A}_\Omega\mathbf{c}\|^2 \tag{5}$$

where λ_ℓ and λ_t are some weights to determine the emphasize on ℓ_1 or TV objective functions, respectively.

To recover a signal from incomplete measurements, the basis $\mathbf{\Phi}$ is fixed and is assumed to be known in advance. Otherwise, one should find $\mathbf{c}$ by guesstimating the basis $\mathbf{\Phi}$. If the results are not satisfying, another basis should be tried and the signal is recovered in the new basis. This procedure is repeated till finding a proper basis which sparsifies the signal well and at the same time is incoherent with the measurement basis. This approach might be very computationally complex and for some applications impossible in practice.

2.2. Best Basis and Dictionary Learning

The problem of selecting a proper basis prior to data recovery using CS is studied in the literature under best basis selection and dictionary learning. The method of best basis compressed sensing is proposed to address the issue of selecting a proper basis in fixed basis compressed sensing [5]. In this approach, the best basis is optimized to obtain the best possible approximation of the signal for a given sparsity. The problem is solved through the unconstrained optimization problem by minimizing a Lagrangian

$$\kappa^* = \arg\min_{\kappa \in \mathrm{K}} \varepsilon\left(c, B^\kappa, t\right)$$
$$\varepsilon\left(c, B^\kappa, t\right) = \min_{\mathbf{c}^\kappa \in \mathrm{C}^\mathrm{N}} \frac{1}{2}\left\|\mathbf{y} - \mathbf{\Phi\Psi c}\right\| + t\left\|\mathbf{c}\right\|_1 \quad (6)$$

where B^κ is an orthonormal basis and t is the Lagrange multiplier. A tree structure is then proposed to produce the set of bases B. While this approach solves the problem of selecting a proper basis, it suffers from high computationally complex algorithm due to optimizing two objective functions at the same time.

A dictionary learning compressed sensing method is proposed in [8] for k-space MR imaging. In this method, the dictionary is adapted to a particular image and at the same time finds out the missing k-space components. A patch-based approach is used for learning the dictionaries. Then, the image is recovered in a two-step alternating scheme. In the first step, the dictionary is updated while the image is kept fixed. In the second step, the dictionary is fixed while the image is updated. Other methods are proposed in [9] for joint design and optimization for learning the dictionary and measurement matrix. In this approach training data set are used for simultaneous learning of sparse representation and measurement matrix.

3. ADAPTIVE BASIS SELECTION (ABS) COMPRESSED SENSING

In this section we introduce the proposed adaptive basis selection compressed sensing method. In this method, the proper basis is selected from a set of bases based on the proposed decision metric. The signal is then recovered using ℓ_1 norm minimization with an iterative approach. In each iteration of the signal recovery, a more accurate estimation of the desired signal is available. Consequently, the decision metric can estimate the proper metric more accurately and will cause the algorithm to switch to a new basis if the initial guess is not the best one. As the signal is evolved during the iterations, the basis keeps updating till the algorithm converges.

In this section, we discuss the proposed ABS compressed sensing method and the proposed strategy to solve the problem. To solve the problem, we propose an algorithm based on alternating direction method (ADM). We also discuss the computational complexity of the proposed algorithm and compare it with the complexity of the existing fixed basis methods. Finally, we propose a practical decision metric to be used with adaptive basis selection method.

3.1. Strategy

Consider a set of N_K bases $\mathbf{B} = \left\{\mathbf{\Psi}^\kappa\right\}_{\kappa \in K}, K = \{1,2,\cdots,N_K\}$ with the κ-th orthogonal basis denoted as $\mathbf{\Psi}^\kappa$. The signal $\mathbf{f}$ can be represented in each $\mathbf{\Psi}^\kappa$ basis as $\mathbf{c}^\kappa$ with support set T^κ of size $\left|T^\kappa\right| = S^\kappa$. The best basis to recover the signal from incomplete measurements $\mathbf{y}$ is the $\mathbf{\Psi}^\kappa$ with the smallest S^κ. But, before solving(3), we have no *a priori* knowledge of which $\mathbf{\Psi}^\kappa$ to choose for a given incomplete measurement.

We define η as

$$\eta\left(\mathbf{c}^\kappa\right) = \mu^2\left(\mathbf{\Phi}, \mathbf{\Psi}^\kappa\right)\left|T^\kappa\right|. \quad (7)$$

This metric can be considered as a measure of how good a sparsifying basis candidate $\mathbf{\Psi}^\kappa$ is able to recover the signal and plays the role of a decision metric. Therefore, during the recovery process (3) by searching for the smallest η, we will come up with the best sparse representation κ^* in the set K

$$\kappa^* = \arg\min_{\kappa \in K} \eta\left(\mathbf{c}^\kappa\right). \quad (8)$$

Finding the best sparse representation is usually inaccurate by using the incomplete measurements. However, this search can result in more accurate results if it is performed iteratively while solving (3) or (5). In this paper we proposed a new iterative algorithm which solves (3) or (5) and at the same time finds the best basis using (8).

We assume that the signal is sampled with a random sequence of $\delta_1, \delta_2, \cdots, \delta_N$ independent identically distributed Bernoulli distribution with

$$p\left(\delta_\kappa\right) = \frac{M}{N} \quad (9)$$

The measurement matrix $\mathbf{\Phi}_\Omega$ is then produced by the rows of the identity matrix randomly sampled on the set Ω.

The proposed algorithm benefits from the capability of adding diversity to the set of bases for a better recovery of an unknown signal. In this way, the sparsifying basis is not limited to any class of basis and different classes could be compared with same metric. For example, discrete Fourier transform and discrete cosine transform sparsify highly oscillating images very well. On the other hand, wavelet-based transforms are more suitable for images which are sparsely represented with spatial-frequency transforms. As the set of bases $\mathbf{A}$ is arbitrary and is completely user defined, the proposed algorithm is able to select from a diverse sets of bases. This property is in contrast to other basis selecting compressed sensing algorithms such as [5] which require searching through one class of dictionary to avoid computational complexity overhead.

3.2. Proposed ABS Algorithm

In this section we introduce the proposed algorithm for solving the adaptive basis selection compressed sensing. The algorithm is based on iteratively solving the basis pursuit problem and updating the sparsifying basis in each iteration based on the sparsity information of the signal. As the algorithm goes through the iterations, a better approximation of the original signal increases the chance of selecting the proper sparsifying basis. Reciprocally, selecting the proper sparsifying basis leads to a higher chance of recovery.

Algorithm 1 shows the iterative procedure for solving the proposed method where I_e is an integer and is a user defined parameter for stopping the basis update procedure. If the sparsifying basis is kept unchanged for I_e iterations, the algorithm stops updating the basis to decrease the overall computational complexity of the recovery process. Typically, I_e is a small number and the basis update procedure stops after the first few iterations.

Algorithm 1 Adaptive Basis Selection (ABS)

1: $\kappa_0 \coloneqq \arg\min \eta\left(\left(\mathbf{A}_\Omega^{\kappa}\right)^H \mathbf{y}\right)$
2: $\mathbf{c}_0 \coloneqq \left(\mathbf{A}_\Omega^{\kappa_0}\right)^H \mathbf{y}$
3: $i \coloneqq 0$
4: **repeat**
5: Update $c_{i+1}^{\kappa_i}$ based on $c_i^{\kappa_i}$
6: **if** κ is changed during last I_e consecutive iterations **then**
7: $\kappa_{i+1} := \arg\min_{\kappa \in K} \eta(\mathbf{c}_{i+1}^{\kappa})$
8: $\mathbf{c}_{i+1}^{\kappa_{i+1}} := (\mathbf{\Psi}^{\kappa_{i+1}})^H \mathbf{\Psi}^{\kappa_i} \mathbf{c}_{i+1}^{\kappa_i}$
9: **else**
10: $\kappa_{i+1} := \kappa_i$
11: $\mathbf{c}_{i+1}^{\kappa_{i+1}} := \mathbf{c}_{i+1}^{\kappa_i}$
12: **endif**
13: $i := i + 1$
14: **until** Stopping criteria is met

An iterative algorithm is developed to investigate the performance of the proposed method. The algorithm uses alternating direction method (ADM) as proposed in [14] to solve the ℓ_1 minimization problem.

According to the general framework of ADM, the augmented Lagrangian sub-problem of (3) for a given $\kappa \in K$ is

$$\begin{aligned} &\min_{\mathbf{c}^\kappa \in \mathbb{C}^N} \lambda_\ell \left\|\mathbf{c}^\kappa\right\|_1 + \lambda_{\mathrm{t}} \mathrm{TV}(\mathbf{\Psi}^\kappa \mathbf{c}^\kappa)\ell_1 \\ &+\mathrm{Re}(\mathbf{z}^H(\mathbf{A}^\kappa \mathbf{c}^\kappa - \mathbf{y})) + \tfrac{\beta}{2}\|\mathbf{A}^\kappa \mathbf{c}^\kappa - \mathbf{y}\|^2 \end{aligned} \tag{10}$$

where $\mathbf{z} \in \mathbb{C}^M$ is a multiplier and $\beta > 0$ is a penalty parameter. Reformulating (10), we have

$$\begin{aligned} &\min_{\mathbf{c}^\kappa \in \mathbb{C}^N} \lambda_\ell \left\|\mathbf{c}^\kappa\right\|_1 + \lambda_{\mathrm{t}} \mathrm{TV}(\mathbf{\Psi}^\kappa \mathbf{c}^\kappa) \\ &+\tfrac{\beta}{2}\|\mathbf{A}^\kappa \mathbf{c}^\kappa - \mathbf{y} - \mathbf{z}/\beta\|^2. \end{aligned} \tag{11}$$

The proposed method as in Algorithm 1 with ADM approach can be approximated to

$$\begin{aligned} &\kappa_i = \arg\min_{\kappa \in K} \eta(\mathbf{c}_{i-1}^{\kappa}) \\ &\min_{\mathbf{c}^{\kappa_i} \in \mathbb{C}^N} \lambda_\ell \left\|\mathbf{c}^{\kappa}\right\|_1 + \lambda_{\mathrm{t}} \mathrm{TV}(\mathbf{\Psi}^\kappa \mathbf{c}^\kappa) \\ &+\beta\left(\mathrm{Re}(\nabla_i^H(\mathbf{c}^{\kappa_i} - \mathbf{c}_i^{\kappa_i})) + \tfrac{1}{2\tau}\|\mathbf{c}^{\kappa_i} - \mathbf{c}_i^{\kappa_i}\|^2\right) \end{aligned} \tag{12}$$

where $\tau > 0$ is a proximal parameter and

$$\nabla_i \triangleq (\mathbf{A}_\Omega^\kappa)^H(\mathbf{A}_\Omega^\kappa \mathbf{c}_i^\kappa - \mathbf{y} - \mathbf{z}_i/\beta) \tag{13}$$

is the gradient of the quadratic term in (11) at point $\mathbf{c}_i^{\kappa_i}$ with i indicating the iteration number. To solve the problem without TV penalty, we can simply set $\lambda_\ell = 1$ and $\lambda_{\mathrm{t}} = 0$. The minimization (12) can be explicitly solved by

$$\begin{aligned} \mathbf{c}_{i+1}^{\kappa_i} &= \mathrm{shrink}\left(\mathbf{c}_i^{\kappa_i} - \tau\nabla_i, \tfrac{\tau}{\beta}\right) \\ &\triangleq \max\left(|\mathbf{c}_i^{\kappa_i} - \tau\nabla_i| - \tfrac{\tau}{\beta}, 0\right) \tfrac{\mathbf{c}_i^{\kappa_i} - \tau\nabla_i}{|\mathbf{c}_i^{\kappa_i} - \tau\nabla_i|} \end{aligned} \tag{14}$$

with all of the operations being performed element-wise. Line 5 of Algorithm 1 is then substituted by the following two lines

$\mathbf{c}_{i+1}^{\kappa_i} := \mathrm{shrink}(\mathbf{c}_i^{\kappa_i} - \nabla_i, \tau/\beta)$
$\mathbf{z}_{i+1} := \mathbf{z}_i - \xi\beta(\mathbf{A}_\Omega^{\kappa_i}\mathbf{c}_{i+1}^{\kappa_i} - \mathbf{y})$

where $\xi > 0$ is a constant.

3.3. Computational Complexity

In this section, we discuss the computational complexity of the proposed algorithms and will compare it with that of fixed basis compressed sensing. Both for fixed basis compressed sensing and proposed method, it is a common practice to calculate the matrix multiplication $\mathbf{f} = \mathbf{\Psi}^\kappa \mathbf{c}$ with an implicit function. Let us assume that the computing time of this implicit function is $X^\kappa(N)$ with biggest order of computation $\mathcal{O}(X^\kappa(N))$ or simply $\mathcal{O}^\kappa$.

The order of computations per iteration for fixed basis compressed sensing using ADM approach is $2\mathcal{O}^\kappa$, where $\kappa \in K$ is a candidate basis. By repeating the recovery process using all bases and finding the best recovered signal, the order of computations will be $2\sum_{\kappa=1}^{|K|} \mathcal{O}^\kappa$. This is while the order of computations for the proposed adaptive basis selection method using ADM approach is $\mathcal{O}^{\kappa_{i+1}} + 2\mathcal{O}^{\kappa_i} + \sum_{\kappa=1}^{|K|} \mathcal{O}^\kappa$ for $i \leq I_e$ and is $2\mathcal{O}^{\kappa^\star}$ for $i > I_e$. To compare the complexity of fixed basis CS with ABS, assume that we sort the bases, $\kappa \in \{1, 2, \cdots, |K|\}$, with respect to their order of complexity with ascending order. The worst case for ABS occurs when the best basis in the set has the highest order of complexity, $\mathcal{O}^{|K|}$. In practice, for $|K| > 3$, the order of complexity per iteration for ABS is less than that of fixed basis applied on all bases. In other words, if the number of candidate bases is larger than three, ABS needs fewer computations than fixed bases repeated for all bases. Note that this is the worst case study and if the best basis is not the most complex one, the order of computations of ABS might be much less than fixed basis. Also, the basis updating procedure stops after I_e iterations.

Assume that fixed basis CS using $\kappa \in K$ candidate basis converges in I^κ iterations. The overall computational time for all bases is then $2\sum_{\kappa=1}^{|K|} \mathcal{O}^\kappa I^\kappa$. On the other hand, ABS converges in $I^{\kappa^\star} + I_e$ with $\kappa^\star$ being the best candidate basis and I_e being the number of iterations needed to find the best basis. Therefore, the overall computational time for worst case study of ABS algorithm is

$\left(3\mathcal{O}^{|K|} + \sum_{\kappa=1}^{|K|} \mathcal{O}^{\kappa}\right) I_e + 2\mathcal{O}^{\kappa^\star} I^{\kappa^\star}$. In practice, $I_e \ll I^{\kappa}, \forall \kappa \in K$ and the overall complexity of the proposed algorithm is much less than the fixed basis algorithm repeated over different bases.

3.4. Measures of Sparsity

As discussed earlier, the sparsity of a signal plays a critical role in performance of data recovery techniques. In practice, most signals have S significant coefficients and the rest of coefficients are close to zero, but not exactly zero. The ℓ_1-norm optimization is capable of recovering these kinds of signals with good approximation despite they are not strictly sparse as defined in (1). Therefore, the definition of sparsity as in (1) is not a proper measure of sparsity in practical.

Several measures of sparsity are proposed in the literature to measure the sparsity of a signal for practical purposes [15]-[17]. These measures include ℓ_p-norm, kurtosis, impulsiveness, pq-mean, and Gini index. After evaluating these measures of sparsity, we selected impulsiveness based on its reliability and computational complexity. As the sparsity increases, impulsiveness of the signal increases. Gini index is also a reliable measure of sparsity [15]-[18], but it has higher computational complexity. As ABS selects the best basis in each iteration based on the measure of sparsity, we need a low complexity measure and Gini index is not suitable for this application.

Impulsiveness is typically used in characterization of impulsive noises and is defined as [19]

$$\gamma_{im}(\mathbf{c}^{\kappa}) = \frac{E\{|c_r^{\kappa}|^2\}^{\frac{1}{2}}}{E\{|c_r^{\kappa}|\}}. \tag{15}$$

When the exact statistics of c_r's are not available, the estimate of impulsiveness reduces to special case of pq-mean with $p = 2$ and $q = 1$ defined as

$$\gamma_{pq}(\mathbf{c}^{\kappa}) = \frac{(\frac{1}{N}\sum_{r=1}^{N}|c_r^{\kappa}|^p)^{\frac{1}{p}}}{(\frac{1}{N}\sum_{r=1}^{N}|c_r^{\kappa}|^q)^{\frac{1}{q}}} \qquad p < q \tag{16}$$

where the negative sign is removed from the definition to make the sparsity measure positive.

It should be noted that all c_r's must be available to calculate these measures of sparsity. However in compressed sensing applications, only incomplete measurements are available. Therefore, we need to estimate the measure of sparsity from incomplete set of data.

In this paper, the measurement method is spatial sampling for which the measurement matrix is a matrix of spikes. We have noticed that for spatial sampling bilinear interpolation of the signal results in the best estimate of measures of sparsity.

3.5. Coherence

Besides sparsity, coherence between the measurement matrix and transform matrix is one of the factors which determine the sufficient number of samples to recover a signal [2], [12]. In this paper, we proposed a decision metric based on both sparsity and coherence (4), to select between different bases. The metric is defined as

$$\tilde{\eta}(\mathbf{c}^{\kappa})^{\kappa} = \frac{\mu^2(\mathbf{\Phi}, \mathbf{\Psi}^{\kappa})}{\gamma(\mathbf{c}^{\kappa})} \tag{17}$$

4. APPLICATION TO WIDEBAND 2D SYNTHETIC APERTURE RADAR IMAGING

In this section, the application of the proposed method for synthetic aperture radar (SAR) imaging for nondestructive testing of materials is discussed and the results are presented. For SAR imaging application, the hardware system performs the measurement in spatial domain and the measurement matrix is a matrix of spikes. Five transform bases are selected to show the performance of the proposed algorithm. The selected bases are: 2D SAR, 2D discrete Fourier transform (DFT), 2D discrete cosine transform (DCT), 2D Daubechies 1 wavelet with one level decomposition (DB1(1)), and 2D DB1 with two level decomposition (DB1(2)). Table 1 lists the set of bases which are used in this paper.

Table 1: Set of bases

Basis	1	2	3	4	5
	SAR	DFT	DCT	DB1 (1)	DB1 (2)

4.1. Synthetic Aperture Radar Imaging

Microwave synthetic aperture radar (SAR) imaging is a nondestructive method for inspecting materials and detecting defects and discontinuities in critical structures. Conventionally, a specimen under test (SUT) is raster scanned with an antenna probe to form high resolution images of the SUT. The cost of high resolution images is the time spent for scanning and acquiring the data with very small spatial steps.

In SAR imaging, a microwave probe illuminates an area of SUT and the hardware device measures the backscattered complex valued reflection coefficients, $\mathbf{f}(x', y', \omega_s)$, which are the superposition of reflections from all points in the illuminated area with x' and y' being the probe location and ω_s being the swept temporal angular frequency. The reflection coefficients

$$\mathbf{f}(x', y', \omega_s) = \iint \mathbf{s}(x, y, \omega_s, z_t) \mathrm{e}^{-j2k_s\sqrt{(x-x')^2+(y-y')^2+z_t^2}}\, \mathrm{d}x\, \mathrm{d}y \tag{18}$$

are superposition of reflections from all points in the illuminated area where $k_s = \frac{\omega_s}{c}$ is the wavenumber and $\mathbf{s}(x, y, \omega_s, z_t)$ is the reflectivity function of the target at location x and y and distance z_t from the probe.

After decomposing the spherical wave propagation into a superposition of plane wave components and dropping the distinction between primed and unprimed coordinates, the estimate of the range migration formula becomes

$$\mathbf{s}(x,y,\omega_s,z_t) = \mathcal{F}_{2D}^{-1}\left\{\mathcal{F}_{2D}\left\{\mathbf{f}(x,y,\omega_s)\right\}\mathrm{e}^{-jz_t\sqrt{4k_s^2-k_x^2-k_y^2}}\right\} \quad (19)$$

where $\mathcal{F}_{2D}\{.\}$ and $\mathcal{F}_{2D}^{-1}\{.\}$ are the 2D Fourier and inverse Fourier transform operators, respectively, k_x and k_y are the Fourier transform variables corresponding to x and y, respectively, and c is the speed of light [20]-[23]. To improve the quality of images, the reflection coefficients, $\mathbf{f}(x,y,\omega_s)$, are measured for a range of frequencies. Then, all focused images are averaged for a given distance of the probe to the target z_t,

$$\mathbf{s}(x,y,z_t) = \frac{1}{N_\omega}\sum_{s=1}^{N_\omega}\mathbf{s}(x,y,\omega_s,z_t) \quad (20)$$

where N_ω is the number of frequency points.

The scan time can be reduced by randomly selecting spatial acquisition points from a uniform grid and optimizing the scan path to minimize the total traveling distance. In compressed sensing SAR imaging technique, the reflection coefficients are sampled randomly from a uniform grid along X and Y dimensions. Then, CS is exploited to recover the uniform grid data and (19) and (20) are used to form 2D images of the target at different heights [10], [11].

The 2D SAR transform is calculated using (19) and can be expressed in matrix format

$$\mathbf{\Psi}_{SAR} = \mathbf{\Psi}_{2DFT}^{H} \times (\mathbf{E} \circ \mathbf{\Psi}_{2DFT}) \quad (21)$$

where $\times$ denotes the matrix product, $\circ$ denotes the Hadamard product, $\mathbf{\Psi}_{SAR}$ is the 2D SAR matrix, and $\mathbf{\Psi}_{2DFT}$ is the 2D Fourier transform matrix and is formed by

$$\mathbf{\Psi}_{2DFT} = \mathbf{\Psi}_{FT} \otimes \mathbf{\Psi}_{FT} \quad (22)$$

where $\otimes$ denotes Kronecker product and $\mathbf{\Psi}_{FT}$ is the 1D Fourier transform matrix. The exponential term in (19) is denoted by matrix $\mathbf{E}$ and is calculated as

$$\mathbf{E}(s,t) = \bar{\mathbf{e}} \otimes \begin{bmatrix} 1 & 1 & \cdots & 1 \end{bmatrix}_{1\times N} \quad (23)$$

where

$$\bar{\mathbf{e}} = \begin{bmatrix} \mathbf{e}_1^T & \mathbf{e}_2^T & \cdots & \mathbf{e}_l^T \end{bmatrix}^T \quad (24)$$

with $\mathbf{e}_l$ being the columns of matrix $\mathbf{e}$ defined as

$$\mathbf{e}_{mn}(s,t) = \left[e^{-jz_t\sqrt{4k_s^2-k_{xm}^2-k_{yn}^2}}\right]_{mn}. \quad (25)$$

The 2D transform matrices for other bases are Kronecker product of 1D bases

$$\mathbf{\Psi}_{2D} = \mathbf{\Psi}_{1D} \otimes \mathbf{\Psi}_{1D} \quad (26)$$

where $\mathbf{\Psi}_{1D}$ is the 1D basis matrix corresponding to each 2D basis matrix, $\mathbf{\Psi}_{2D}$.

4.2. Results

The goal in adaptive basis selection compressed sensing SAR imaging is to find a proper sparse representation of $\mathbf{f}(x,y,\omega_s)$ from incomplete measured reflection coefficients, $\mathbf{y}(x,y,\omega_s)$. The hardware system is designed to randomly measure the reflection coefficients and the *a priori* knowledge of proper representation is not available from incomplete data. On the other hand, the proper sparse representation might be different for different SUTs. Using the proposed algorithm, the proper representation is selected adaptively as the signal is evolved during the recovery process. Spatial sampling is selected for SAR imaging because of hardware specifications. Therefore, the decision metric is based on bilinear interpolation of $\mathbf{y}(x,y,\omega_s)$'s.

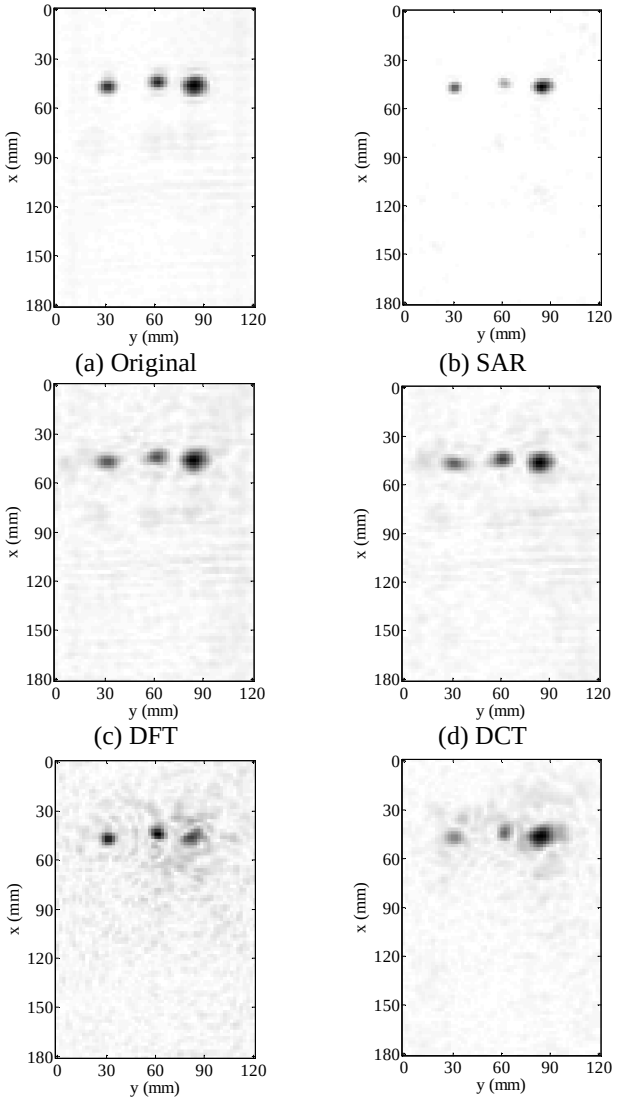

Fig. 1: 2D SAR images of the SUT from complete data and recovered using fixed bases from 20% randomly selected points at z=-28.

To show the efficiency of the proposed method, experimental test were conducted on an SUT which was eight rubber (Rbr) patches and one copper (Cu) patch fixed on a substrate at different heights using pieces of construction foams as physical support. The imaging probe is operating at 18 GHz to 26.5 GHz with frequency steps of 0.6 GHz. An area of $120 \times 180\mathrm{mm}^2$ is scanned and the reflections are received

by the same antenna probe. The complex-valued reflection coefficients are measured and recorded by an HP 8510C vector network analyzer.

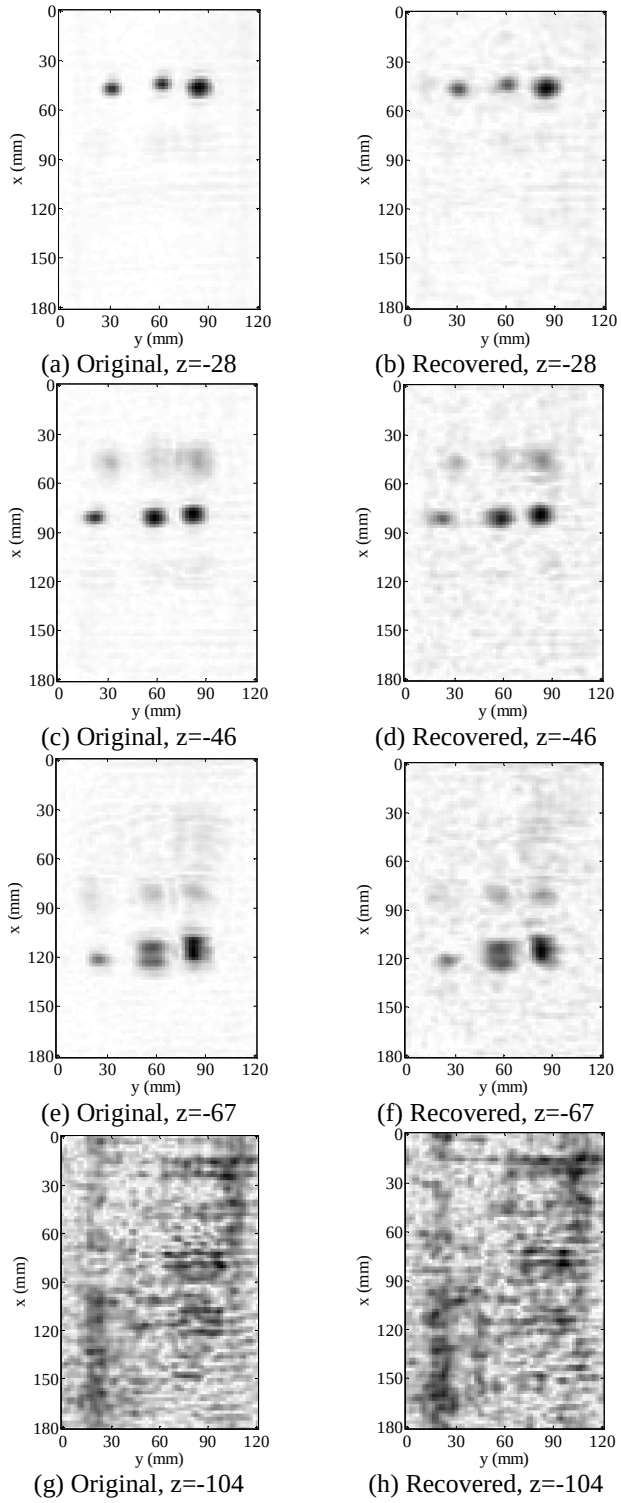

(a) Original, z=-28 (b) Recovered, z=-28

(c) Original, z=-46 (d) Recovered, z=-46

(e) Original, z=-67 (f) Recovered, z=-67

(g) Original, z=-104 (h) Recovered, z=-104

Fig. 2: 2D SAR images of the SUT from complete data and recovered data from 20% randomly selected points using ABS.

The ADM approach is used to recover the SAR images. To see the effect of sparsifying basis on signal recovery, we have recovered SAR images using different bases. The results of the recovered images for $z = -28$ are shown in Fig. 1. It can be seen that different bases have recovered the images with different qualities. The closest one in terms of normalized root mean square (NRMS) error to the original image with complete measurement points is the one recovered using 2D DFT basis. The worse basis in terms of error is 2D DB1(1).

The same SAR images are recovered using the proposed algorithm with the ADM approach. The algorithm has detected the sparsest basis for all pairs of (ω_s, z_t) correctly and has evolved the signal in the correct basis. The resulting 2D compressed sensing SAR images of the SUT using the proposed method is shown in Fig. 2 with 20% of the points used in the complete data. These figures show the SAR images focused on three different levels of the targets and images from substrate level.

The convergence of the proposed algorithm is studied for this set of images. Figure 3 illustrates the error and the decision metric behavior of the algorithm on the same plot. It can be seen that as the algorithm converges, it selects the best basis (DFT) and converges to the desired signal with this basis. The algorithm also selects DB1(1) as the worst basis and sorts all other bases in between these two bases. The initial guess for the sparsifying basis is based on initialization in Algorithm 1.

The robustness of the algorithm to initial basis is studied by forcing the algorithm to select a wrong initial basis. Figure 4 shows how the algorithm selects the best basis with different initialization. The numbers on the vertical axis indicate the bases according to Table 1. The maximum number of iterations for basis convergence, I_e, is 20. From the figure, it can be seen that the algorithm selects the best basis after the first iteration for all basis except SAR. When the sparsifying transform is selected as SAR for initialization, the algorithm selects SAR after 7 iterations as the best basis which is the second best basis in the set of bases.

5. CONCLUSION

Recently developed compressed sensing theory has proposed a more efficient acquisition of signals by sampling below conventional Nyquist rate. However, there is a need for selecting a proper basis for recovering of signals using sparse representation. This is while no *a priori* knowledge of the proper basis is available before the signal is recovered. On the other hand, the proper basis should be selected based on incomplete measurements.

In this paper we proposed a low computationally complex algorithm called adaptive basis selection compressed sensing to recover images from incomplete measurement without any knowledge of the proper sparse representation. To detect the best basis from a set of bases, a decision metric is introduced to select between the bases as the signal is evolved during the iterations of the algorithm. The 2D synthetic aperture radar images were used in this paper to show the performance of the

proposed method. The results of our experiments showed that the proposed algorithm successfully selected the best basis adaptively and was capable of recovering the images with high accuracy.

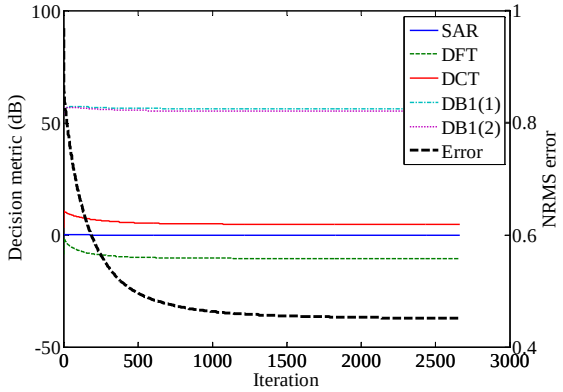

Fig. 3: Decision metric and error vs. number of iterations for SAR data.

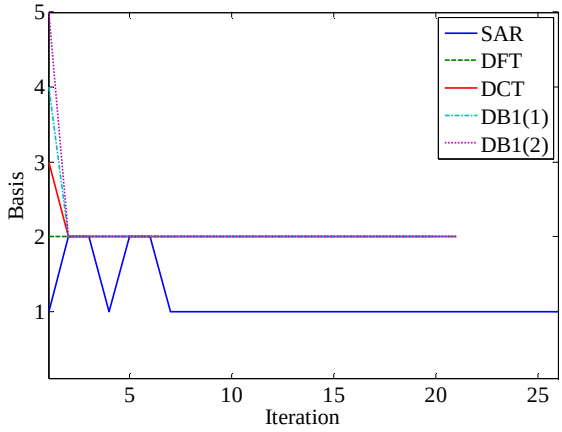

Fig. 4: Basis convergence vs. number of iterations for SAR data for different basis initialization.

6. ACKNOWLEDGMENT

We wish to thank Dr. Sergey Kharkovsky and Dr. Reza Zoughi for their valuable assistance in setting up the measurement apparatus. This work was partially supported by Intelligent Systems Center, the ASNT fellowship award, and the University of Missouri Research Board fund.

7. REFERENCES

[1] Donoho, D.L., 2006, "Compressed sensing," IEEE Trans. Inf. Theory, 52(4), pp. 1289-1306.

[2] Candes, E.J., Romberg, J., and Tao, T., 2006, "Robust uncertainty principles: exact signal reconstruction from highly incomplete frequency information," IEEE Trans. Inf. Theory, 52(2), pp. 489-509.

[3] Candes, E.J., and Wakin, M.B., 2008, "An introduction to compressive sampling," IEEE Signal Process. Mag., 25(2), pp. 21-30.

[4] Duarte-Carvajalino, J.M., and Sapiro, G., 2009, "Learning to sense sparse signals: Simultaneous sensing matrix and sparsifying dictionary optimization," IEEE Trans. Image Process., 18(7), pp. 1395-1408.

[5] Peyre, G., 2010, "Best basis compressed sensing," IEEE Trans. Signal Process., 58(5), pp. 2613-2622.

[6] Chen, H.W., Kang, L.W., and Lu, C.S., 2012, "Dictionary learning-based distributed compressive video sensing," Picture Coding Symp. (PCS), pp. 210-213.

[7] Soni, A., and Haupt, J., 2011, "Efficient adaptive compressive sensing using sparse hierarchical learned dictionaries," ArXiv e-prints, pp. 1-5.

[8] Ravishankar, S., and Bresler, Y., 2011, "MR image reconstruction from highly undersampled k-space data by dictionary learning," IEEE Trans. Med. Imag., 30(5), pp. 1028-1041.

[9] Thiagarajan, J.J., Ramamurthy, K.N., and Spanias, A., 2011, "Multilevel dictionary learning for sparse representation of images," Digital Signal Processing Workshop and IEEE Signal Processing Education Workshop (DSP/SPE), pp. 271-276.

[10] Kajbaf, H., Case, J.T., Zheng, Y.R., Kharkovsky, S., and Zoughi, R., 2011, "Quantitative and qualitative comparison of SAR images from incomplete measurements using compressed sensing and nonuniform FFT," Proc. 2011 IEEE Radar Conf. (RADAR), Kansas City, MO, pp. 592-596.

[11] Kajbaf, H., Case, J.T., Zheng, Y.R., 2011, "3D image reconstruction from sparse measurement of wideband millimeter wave SAR Experiments," Proc. of the 18th IEEE Int. Conf. on Image Process. (IEEE ICIP 2011), Brussels, Belgium, pp. 2701-2704.

[12] Candes, E.J., and Romberg, J., 2007, "Sparsity and incoherence in compressive sampling," Inverse Prob., 23(3), pp. 969-985.

[13] Lustig, M., Donoho, D.L., and Pauly, J.M., 2007, "Sparse MRI: the application of compressed sensing for rapid MR imaging," Magn. Reson. Med., 58(6), pp. 1182-1195.

[14] Yang, J., and Zhang, Y., 2010, "Alternating algorithms for L1-problems in compressive sensing," Rice University CAAM, Tech. Rep. TR09-37.

[15] Rickard, S.¸ 2006, "Sparse sources are separated sources," Proc. 16th Annu. European Signal Process. Conf., Florence, Italy.

[16] Akujuobi, C.M., Odejide, O.O., Annamalai, A., and Fudge, G.L., 2007, "Sparseness measures of signals for compressive sampling,"IEEE Int. Symp. on Signal Process. and Inform. Technology, pp. 1042-1047.

[17] Hurley, N., and Rickard, S., 2009, "Comparing measures of sparsity," IEEE Trans. Inf. Theory, 55(10), pp. 4723-4741.

[18] Zonoobi, D., Kassim, A.A., and Venkatesh, Y.V., 2011, "Gini index as sparsity measure for signal

reconstruction from compressive samples," IEEE J. Sel. Topics Signal Process., 5(5), pp. 927-932.
[19] Schonhoff, T.A., and Giordano, A.A., Detection and Estimation Theory and Its Applications, Prentice Hall.
[20] Soumekh, M., 1991, "Bistatic synthetic aperture radar inversion with application in dynamic object imaging," IEEE Trans. Signal Process., 39(9), pp. 2044-2055.
[21] Lopez-Sanchez, J.M., and Fortuny-Guasch, J., 2000, "3-D radar imaging using range migration techniques," IEEE Trans. Antennas Propag., 48(5), pp. 728-737.
[22] Sheen, D.M., McMakin, D.L., and Hall, T.E., 2001, "Three-dimensional millimeter-wave imaging for concealed weapon detection," IEEE Trans. Microw. Theory Tech., 49(9), pp. 1581-1592.
[23] Case, J.T., Kharkovsky, S., Zoughi, R., Steffes, G., Hepburn, F.L., 2008, "Millimeter wave holographical inspection of honeycomb composites," Thompson, D.O., and Chimenti, D.E. (Eds.) `Review of Progress in Quantitative Nondestructive Evaluation Vol. 27B, AIP Conference Proceedings' (American Institute of Physics, Melville, NY, 2008), 975, pp. 970-975.